Chapter 7 - Motility

Both living and inanimate microscopic objects are subject to *thermal fluctuations*, which causes them to jiggle about incessantly when viewed under an optical microscope. Many biological organisms modify these thermal fluctuations to facilitate the transport of the molecules inside their bodies and also to move themselves through their environment. Motility in biological systems is crucially important in a wide range of biological processes that include the transcription of DNA, the packaging of DNA in viruses, the propulsion of bacteria as they search for food and striated muscle as it is exercised (when a dumb bell is lifted or the heart contracts).

Initially an understanding of the undriven process of passive diffusion due to thermal energy will be developed, and this will then be extended to the analysis of motions produced by molecular motors (also see **Chapter 16** on molecular motors). Nanoparticles move as if caught in a randomly fluctuating hurricane and nanomotors are presented with a series of challenges to perform directed motion in this stochastic hurricane. Even more curious are the fluid mechanics effects due to the small length scales involved. Fluid dynamics occur at low Reynolds number, so inertial forces are negligible. Thus the directed motion of biological molecules in the stochastic hurricane occurs in a watery environment that acts like treacle on the nanoscale.

Due to the importance of motility for the determination of biological processes, a series of non-invasive methods have been developed to measure molecular motility (**Chapter 19**), which include fluorescence correlation spectroscopy, pulsed femtosecond laser techniques, dynamic light scattering, neutron/X-ray inelastic scattering, video particle tracking, and nuclear magnetic resonance spectroscopy. Based on this wide range of dynamic techniques the field of biological motility has been provided with firm experimental foundations. The time scales that are now routinely experimentally probed range from femtoseconds (10^{-15} s) with biomolecular liquids, all the way up to the aging processes of biopolymer glasses, which are on the order of many years.

7.1) Diffusion

Diffusion is the process by which molecules jiggle around at small length scales due to thermal collisions with their neighbours, and equivalently, diffusion can be used to explain how macroscopic concentration gradients in materials evolve with time. Thus a food dye injected into water eventually colours the whole vessel as the dye diffuses throughout the specimen; the jiggling motion at the nanometre scale produces a global redistribution of the dye molecules at the macroscale. To obtain a quantitative understanding of the process of diffusion, it will first be described in a statistical way at short length scales; the phenomenon of *Brownian motion*. At the macroscopic level an equivalent description is provided by *Fick's laws* for the concentration of a diffusing species.

As a first step it is useful to examine the statistical form of translational diffusion in one dimension, since it simplifies the analysis. A particle takes random steps to the left and to the right. In one dimension the displacement ($x_i(n)$) of a single diffusing particle as a function of the position of the previous random displacement ($x_i(n-1)$) after n steps is

$$x_i(n) = x_i(n-1) \pm \delta \qquad (7.1)$$

where δ is the step size, which is assumed constant (this assumption can be relaxed using a Gaussian distribution of step sizes, but does not affect the final result), and n is the number of steps. The average of the displacements (x_i) is zero ($\langle x_i(n)\rangle = 0$), so the square of this quantity needs to be used to create a meaningful measure of the particle's motion,

$$x_i^2(n) = x_i^2(n-1) \pm 2\delta x_i(n-1) + \delta^2 \qquad (7.2)$$

Next the mean square value of the displacement can be constructed and the second term in (7.2) averages to zero, since $\langle x_i(n-1)\rangle = 0$. Therefore the mean square displacement ($\langle x^2(n)\rangle$) is given by

$$\left\langle x^2(n)\right\rangle = \frac{1}{N}\sum_{i=1}^{n} x_i^2(n) = \left\langle x^2(n-1)\right\rangle + \delta^2 \qquad (7.3)$$

This expression for the mean square displacement is an iterative equation that relates the mean square displacement at step n ($\langle x_i^2(n)\rangle$) to that of the previous step ($\langle x_i^2(n-1)\rangle$). The application of equation (7.3) can be iterated all the way down to the first step of the motion ($n=1$) and it is seen that the mean square displacement scales as the number of time steps (n) i.e.

$$\left\langle x^2(n)\right\rangle = n\delta^2 \qquad (7.4)$$

where n is proportional to the time (t). This linear scaling of the mean square displacement with the time is a basic characteristic of diffusive motion. The number of time steps is related to the time (t) and the step size (τ). Thus the number of steps is given by $n=t/\tau$ and this expression can be substituted in equation (7.4) to give

$$\left\langle x^2(t)\right\rangle = \left(\frac{\delta^2}{\tau}\right)t \qquad (7.5)$$

The *diffusion coefficient* (D) is then defined to quantify the magnitude of the particle's mean square displacement fluctuations,

$$D = \frac{\delta^2}{2\tau} \qquad (7.6)$$

Particles with large diffusion coefficients fluctuate a lot and vice versa. The factor of a ½ in equation (7.6) is used to tidy up Fick's equation in the corresponding macroscopic continuum description (equation (7.17)). Combination of equations (7.5) and (7.6) gives an expression that relates the diffusion coefficient to the mean square fluctuations of displacement in *one dimension*,

$$\left\langle x^2(t)\right\rangle = 2Dt \qquad (7.7)$$

Diffusion in one dimension statistically corresponds to the probability distribution of the particle positions broadening with time (**figure 7.1**).A well localised point-like distribution of particles at the first time step ($t=1$) evolves into a broad distribution ($t=15$) as the diffusive motion takes place. Units of diffusion are m^2s^{-1}, quite different to that of velocity, ms^{-1}. A velocity is not defined, because its value would depend on the time scale of observation, and is thus not a particularly meaningful quantity.

For a small molecule in water at room temperature a typical diffusion coefficient (D) is 10^{-5} cm^2s^{-1}. The characteristic time for this molecule to diffuse the length of a bacterium (10^{-4} cm) is then $t \approx x^2/2D = 5\times10^{-4}$ s from equation (7.7).

For *two* or *three dimensions* the extension of the definition of the diffusion coefficient is fairly simple,

$$\left\langle r^2\right\rangle = 2pDt \qquad (7.8)$$

where r is the displacement in p dimensions, t is the time and D is the diffusion coefficient. An example of a two dimensional random walk is shown in **figure 7.2** for a polystyrene sphere moving in water and a more viscous glycerol solution. Clearly an increase in the viscosity of the solution decreases the amplitude of the fluctuations of the displacement of the polystyrene spheres. The decrease in the spheres' fluctuations is explained by the increased friction experienced by the particle in the more viscous fluid. The diffusion coefficient is related to the force of dissipation using the Einstein relationship (the *fluctuation-dissipation theory*),

$$D = \frac{kT}{f} \qquad (7.9)$$

where kT is the thermal energy, D is the diffusion coefficient and f is the frictional coefficient. Something that dissipates a lot fluctuates very little and vice-versa. The generalisation of this expression to viscoelastic materials is considered in **Chapter 15** and an electrical analogue appears in **Chapter 23**.

Newton's law of viscosity states that viscosity quantifies the effect of the shear on the velocity gradient in the fluid i.e.

$$\frac{F}{A} = \eta\frac{v}{d} \qquad (7.10)$$

Thus viscosity (units $Pa\ s$) is the constant of proportionality between the shear stress (F/A, where F is the force and A is the area), and the velocity gradient (v/d, where v is the velocity and d is the plate separation, **Chapter 14**).

For a sphere in a fluid, if non-slip boundary conditions are assumed, the frictional coefficient (f) can be calculated from Navier Stokes equations (**Chapter 14**) and is given by the Stoke's relationship,

$$f = 6\pi\eta a \qquad (7.11)$$

where η is the viscosity of the fluid and a is the particle radius. Friction coefficients are known (or can be numerically calculated) for a wide range of rigid microscopic objects in solution. The *Stokes-Einstein* equation for a sphere combines equations (7.9) and (7.11) to give

$$D = \frac{kT}{6\pi\eta a} \qquad (7.12)$$

Thus measurement of the fluctuations in a particle's position as a function of time (or equivalently the diffusion coefficient) allows the size of the particle to be calculated.

It is important to realise that there is a difference between *mutual-diffusion* and *self-diffusion*. With mutual diffusion the fluctuating rearrangement of particles with respect to their neighbours is considered, whereas with self-diffusion it is the rearrangement of individual particles relative to the laboratory that is important. Experimental techniques are often sensitive to one or other of the two types of diffusion. The previous discussion was centred on *translational self-diffusion* e.g. measured using video particle tracking experiments. Photon correlation spectroscopy experiments often measure translational mutual diffusion.

Particles in solution experience fluctuations in their *rotational motion* in much the same was as with translational motion. The particles are constantly being buffeted by the surrounding solvent molecules, which impart angular momentum to them. A similar statistical analysis is possible for their angular motion as that for translational motion, equations (7.1)-(7.9). The mean square angular rotation ($<\theta^2>$) for small angular rotations (a small angle approximation is used in the derivation) is found to be related to the time (t) through the *rotational diffusion coefficient* (D_θ),

$$\left\langle \theta^2 \right\rangle = nD_\theta t \qquad (7.13)$$

The fluctuation dissipation theory can again be used and in this case it relates the rotational diffusion coefficient to the thermal energy (kT) and the fricitional coefficient (f_θ) for rotational motion,

$$D_\theta = \frac{kT}{f_\theta} \qquad (7.14)$$

For a sphere the frictional coefficient for rotational motion is given by

$$f_\theta = 8\pi\eta a^3 \qquad (7.15)$$

where a is the radius and η is the solvent viscosity. The two equations (7.14) and (7.15) can be combined to provide an expression for the rotational diffusion coefficient of a sphere,

$$D_\theta = \frac{kT}{8\pi\eta a^3} \qquad (7.16)$$

There is a strong dependence of the rotational frictional coefficient on the particle radius (a), and thus large particles rotate very slowly.

There is a macroscopic description of *translational diffusion* which uses Fick's laws and is equivalent to the microscopic approach for translation on small length scales. *Fick's first equation* relates the flux of particles (J_x) that diffuse to the gradient of the particle concentration ($\partial c/\partial x$),

$$J_x = -D\frac{\partial c}{\partial x} \qquad (7.17)$$

where the particle concentration (c) is in moles per cm^3, and the flux is in particles/cm^{2}sec. In words, equation (7.17) states that the net diffusive flux (at both position (x) and time (t)) is proportional to the slope of the concentration function (at both x and t). The constant of proportionality is the negative of the diffusion coefficient ($-D$). Diffusion occurs down concentration gradients.

Fick's second equation is

$$\frac{\partial c}{\partial t} = D\frac{\partial^2 c}{\partial x^2} \qquad (7.18)$$

Again in words, the time rate of change in concentration (at x and t) is proportional to the curvature of the concentration function (at x and t), and the constant of proportionality is again the diffusion coefficient (D). A non-uniform distribution of particles redistributes itself in time according to Fick's two laws. This is pictured in **figure 7.3**, where a sharp concentration gradient in dye molecules is reduced during time by inter-diffusion of the dye and solvent molecules.

In three dimensions Fick's two laws, equations (7.17) and (7.18), can be written in vector notation as

$$\underline{J} = -D\underline{\nabla}c \qquad (7.19)$$

$$\frac{\partial c}{\partial t} = D\nabla^2 c \qquad (7.20)$$

For a quick solution to these partial differential equations in a particular geometry, the most efficient strategy is to look them up in a specialist applied mathematics text book. Solution of such diffusion problems often requires sophisticated mathematical methods i.e. Green's functions. However, some solutions to diffusion in a range of specific geometries will be briefly quoted to give a flavour of the basic principles involved.

a) Diffusion from a *point source*. Consider the injection of some fluorescent dye from a micropipette. The diffusion of the dye is found to be well described by the equation

$$c(r,t) = \frac{N}{(4\pi Dt)^{3/2}} \exp\left(\frac{-r^2}{4Dt}\right) \qquad (7.21)$$

where $c(r,t)$ is the concentration of the dye molecules as a function of time (t), r is distance from the point of injection, and N is the total number of dye molecules. It agrees with the expected result for the microscopic mean square displacement (equation (7.8)) i.e.

$$\left\langle r^2 \right\rangle = \frac{\int_{-\infty}^{\infty} c(r,t) r^2 dx}{N} = 2Dt \qquad (7.22)$$

The flux of dye molecules can then be calculated from Ficks first law, equation (7.19). Experimentally the dye molecules under the microscope first appear as a bright spot upon injection, that spreads rapidly outwards, and then fades away as the concentration becomes homogenised at a low value (**figure 7.1**). **Figure 7.4** shows how the concentration at a single spatial position from a point source evolves with time.

b) Diffusion to a *spherical adsorber*. It is assumed that every particle that reaches the surface of a sphere is gobbled up (**figure 7.5a**). These boundary conditions are slightly artificial (perhaps a good model for a stationary feeding bacterium), but mathematically the concentration at the surface of the sphere ($r=a$) is assumed to be zero and at a long distance from the sphere ($r=\infty$) it is c_0. The solution for the concentration of diffusing particles is found to be

$$c(r) = c_0\left(1 - \frac{a}{r}\right) \qquad (7.23)$$

where a is the radius of the sphere. The flux of diffusive particles can be then calculated from Fick's first law (equation (7.19)),

$$J_r = -D\frac{\partial c}{\partial r} = -Dc_0\frac{a}{r^2} \qquad (7.24)$$

The particles are adsorbed by the sphere at a rate (I) equal to the area ($4\pi a^2$) times the inward flux ($-J_r(a)$) given by equation (7.24),

$$I = 4\pi Dac_0 \qquad (7.25)$$

The adsorption rate (I) is the *diffusion current of particles* per second, and c_0 is the particle concentration per cm^3. Similar results with the current proportional to the size of the particles ($I \sim a$) are found for a wide range of different absorption geometries and thus the rate of capture is relatively independent of the geometry. This implies a wide range of efficient mechanisms are possible in nature for the absorption of biomolecules and this is indeed observed with the feeding strategies of microorganisms. Such considerations with the diffusion equation are also important for a range of reaction diffusion problems (e.g. the Turing model for morphogenesis in **Section 22.9**) and three more results will be quoted for completeness.

c) For diffusion to a *disk-like adsorber* the adsorption rate (**figure 7b**) is

$$I = 4Dsc_0 \qquad (7.26)$$

where s is the diameter of the aperture.

d) For diffusion through a *circular aperture* (**figure 7.5c**) from a particle concentration of c_1 on one side of the aperture to c_2 on the other side of the aperture, the current is

$$I_{2,1} = 2Ds(c_2 - c_1) \qquad (7.27)$$

The currents are not proportional to the area of the disk, but instead depends on its radius (s).

e) For diffusion to an *ellipsoidal adsorber* (**figure 7.5d**) the concentration at the surface of the ellipsoid is zero and the concentration at a large distance of separation ($r=\infty$) is c_0. The length of the major axis of the ellipsoid is a and its minor axis is b. If $a^2>>b^2$ the diffusive current is

$$I = \frac{4\pi D a c_0}{\ln(2a/b)} \qquad (7.28)$$

Again the current is roughly proportional to the length (a).

Often diffusion is not sufficiently fast to transport cargoes inside large cells. Motor proteins are required in this case to reduce the transit times. Even just the partial breakdown of motor protein transport can have serious consequences for the organisms involved e.g. motor neuron disease occurs when the dyneins malfunction that are required to move neurotransmitters along nerve cells (specifically dynactin, a protein that improves dynein's processivity, is implicated in some human motor neuron diseases).

7.2) Low Reynold's number dynamics

The Reynolds number turns up in a number of different guises in fluid mechanics, because a wide range of phenomena depend on the relative importance of frictional effects to inertial effects. Reynolds originally introduced his dimensionless ratio to describe the onset of turbulent flow of a fluid in a pipe. *Laminar flow* occurs at high viscosities (low Reynolds numbers). *Turbulent flow* occurs at low viscosities (high Reynolds numbers). When a fluid is stirred at low Reynolds number it produces the least possible disturbance (laminar flow) and the flow stops immediately after the external force stops. When the Reynolds number is large, inertial effects can dominate e.g. coffee will continue to swirl after stirring is stopped and the flow is turbulent.

In molecular biophysics diffusion predominantly occurs under *low Reynolds number conditions*. This provides some counterintuitive results, since viscous effects dominate the motion and particle inertia is negligible, but the good news is that low Reynolds number conditions greatly simplify the mathematics required to understand the motion of biological molecules at small length scales.

The *Reynolds number* (R, a dimensionless ratio) of a particle that moves at a velocity (v) in a fluid is defined by

$$R = \frac{vL\rho}{\eta} \qquad (7.29)$$

where L is the size of a particle, ρ is the specific gravity (density) of the fluid and η is the viscosity. The utility of the Reynolds number is found through an analysis of Navier-Stokes equations; the equations that predict the general motion of fluids, **Chapter 14**. Navier-Stokes equation for an incompressible fluid is

$$-\nabla p + \eta\nabla^2 v = \rho\frac{\partial v}{\partial t} + \rho(v.\nabla)v \qquad (7.30)$$

where p pressure, v velocity, η viscosity, and ρ density. If $Re<<1$, the time dependence can be neglected in equation (7.30) and the inertial terms on the right can be neglected. The pattern of motion is the same, whether slow or fast, whether forward or backward in time. Practically it is found that when $Re<1$ inertial forces (mdv/dt, where m is the mass) can be neglected at reasonably long time scales (>0.001 s). Furthermore there is no turbulent flow in the system at low Reynolds number. For a salmon that travels at a velocity (v) of 10^2 cms^{-1}, with a length (L) of 10 cm, specific density (ρ) of 1 gcm^{-3}, water viscosity (η) of 10^{-2} $gcm^{-1}s^{-1}$ the Reynolds number is 10^5 (large Reynolds number dynamics). However for a bacterium travelling at $v\approx10^{-3}\ cms^{-1}$, $L=10^{-4}\ cm$, $\rho\approx1\ gcm^{-3}$, $\eta\approx10^{-2}\ gcm^{-1}s^{-1}$ the Reynolds number is very small $R\approx10^{-5}$ (small Reynolds number dynamics). Due to the relative importance of the inertial terms the fish and the bacterium have different strategies for swimming. The salmon propels itself by the acceleration of the water that surrounds it. A bacterium uses viscous shear to propel itself.

A useful example that emphasises the counterintuitive behaviour in low Reynolds number motility is to calculate the length a bacterium can coast before it comes to a stop (**figure 7.6**). The mathematical analysis is very simple. Without any external forces in a purely viscous material, Newton's second law relates the acceleration (dv/dt) to the frictional force created by the relative motion of the surrounding water, equation (7.11). The bacterial is assumed spherical and therefore

$$-m\frac{dv}{dt} = 6\pi\eta a v \qquad (7.31)$$

where m is the mass of the particle, v is the velocity, η is the viscosity of water and a is the particle radius. There is a velocity on both sides of this equation and it can be integrated by parts,

$$\frac{dv}{v} = -\frac{6\pi\eta a}{m}dt \qquad (7.32)$$

Solution of this equation indicates that the velocity relaxes to zero with a characteristic time constant (τ),

$$v(t) = v(0)e^{-t/\tau} \qquad (7.33)$$

$$\tau = \frac{2a^2\rho}{9\eta} \qquad (7.34)$$

where ρ is the density of the bacterium. This result for the velocity can be integrated once more to provide the distance coasted (d) by the bacterium before it comes to a halt,

$$d = \int_0^\infty v(t)dt = v(0)\tau \qquad (7.35)$$

Through substitution of typical values for v, a, ρ and η, the coasting distance of a bacterium is found to be very small, it is 0.04 Å, smaller than the size of a single covalent bond. The stopping distance scales as the square of the particle radius, and thus small particles coast much smaller distances than large particles.

A range of microfluidic experiments depend on the low Reynolds number approximation to interpret the data e.g. microrheology apparatus and optical/magnetic tweezer force measurements at low frequencies (**Chapter 19**). The *Langevin equation* is a useful method for understanding the displacement spectrum of thermally driven motion of a particle. Practically the Langevin equation is encountered in situations such as the fluctuations in the position of an AFM tip or the high frequency fluctuations of the bead position trapped using optical tweezers. The equation for the displacement fluctuations of a particle's motion can be written using Newton's second law,

$$m\frac{d^2x(t)}{dt^2} + \gamma\frac{dx(t)}{dt} + \kappa x(t) = F(t) \qquad (7.36)$$

where $x(t)$ is the particle displacement as a function of time, md^2x/dt^2 is the inertial force that acts on the particle, $\gamma dx/dt$ is the drag force, κx is the elastic force and $F(t)$ is the random force that causes the motion of the particle e.g. driven by thermal energy. It is the introduction of the fluctuating random force that complicates the analysis and gives rise to a separate designation for equation (7.36) as the *Langevin equation*.

The *autocorrelation function* of the displacement ($R_x(\tau)$) of the particle displacement is practically very useful in a range of spectral applications. The autocorrelation function is defined as

$$R_x(\tau) = \langle x(t)x(t-\tau)\rangle = \lim_{T\to\infty}\left\{\frac{1}{T}\int_{-T/2}^{T/2} x(t)x(t-\tau)dt\right\} \qquad (7.37)$$

This autocorrelation function satisfies the equation of motion (7.36) with the simplification that the right hand side is zero, since the displacement (x) and the force (F) are uncorrelated by definition. Substitution of R_x is equation (7.32) gives

$$m\frac{d^2R_x(\tau)}{d\tau^2} + \gamma\frac{dR_x(\tau)}{d\tau} + \kappa R_x(\tau) = 0 \qquad (7.38)$$

Such a second order ordinary differential equation can be solved in the standard manner.

7.3) Motility of cells and microorganisms

The absence of inertial forces could at first site appear to present an insurmountable barrier for a biological organism which needs to propel itself at the micron length scale. Reciprocal motion (e.g. waggling a paddle to and fro) does not lead to motility at the micron scale. It is similar to the case of a human who attempts to do the breath stroke in a swimming pool filled with tar; they move nowhere. Consideration of such behaviour led Ed Purcell to postulate his Scallop theorem (**figure 7.7a**). At low Reynolds number a scallop with a single hinge can move nowhere. In contrast the inclusion of an additional hinge on an organism allows the time symmetry of the motion to be broken and the organism can swim using the gait shown in **figure 7.7b**.

Evolution has overcome the problem of low Reynolds number dynamics in a variety of ways. Propulsion mechanisms most commonly depends on the anisotropy of the drag force on a slender filament. The drag force is two times larger perpendicular to the filament than parallel to it. If a slender filament is moved in a non-reciprocal manner (the forward and backward strokes are different) often the organism is provided with a mechanism for propulsion. Flagellae (from the Latin for whip, where motor proteins at their base cause them to rotate) are used for bacterial propulsion, but another standard mechanism is to use cilia (from the Latin for eye lashes, where motor proteins are distributed along the cilium's length and cause active shape modifications). Cilia are used for micro-organism locomotion (e.g. with protists such as paramecium), but also in the lungs and reproductive tracts of humans (**figure 7.8**). A rod dragged along its axis at velocity $\underline{v}$ feels a resisting force proportional to $-\underline{v}$ (also directed along its axis). Similarly a rod dragged perpendicular to its axis feels a resisting force also proportional to $-\underline{v}$ (directed perpendicular to its axis). However the viscous friction coefficient for motion parallel to the axis is smaller than for perpendicular motion. The motion of the fluid created by a power stroke of a cilium is only partly undone by the backflow created by the recovery stroke and the organism can move. Other examples of motor protein motility are provided in **Chapter 16**.

Flagellated bacterium swim in a manner characteristic of the size and shape of the cell and the number and distribution of the flagellae e.g. an E.coli of 1 μm in diameter and 2 μm in length has six flagellar filaments for propulsion. The flagellae are driven by a particularly elegant device for propulsion; the rotatory motor (**Chapter 16**). The motion of the bacteria is determined by the simultaneous action of the six flagellar filaments. When the flagellae turn counter clockwise they form a synchronous bundle that pushes the body steadily forward; the cell 'runs'. When the filaments turn independently the cell moves erratically and the cell 'tumbles'. The cells switch back and forth between the run and tumble modes of transport at random. The distribution of run (or tumble) intervals is exponential and the length of a given interval does not depend on the length of the intervals that precede it. Using this mechanism the bacteria can search for nutrients in its aqueous environment (**figure 7.9**). This active motion has completely different statistics to the Brownian process depicted in **figure 7.2**; its statistics are Poisson (**Chapter 3**).

Bacterial locomotion is thus achieved by the action of flagellar filaments. The thrust is produced from the component of viscous shear (F_v) of the helical filament on the surrounding water in the direction of motion (**figure 7.10**).

The probability distribution (P) for a Poisson statistical process is given by equation (3.10). Therefore the probability that a particle changes direction once in a time period between t and $t+dt$ is

$$P(t,\lambda) = \lambda e^{-\lambda t} dt \quad (7.39)$$

The probability that there is a change in direction per unit time is λ. The expectation time for the particle to change direction is

$$\langle t \rangle = \frac{1}{\lambda} \quad (7.40)$$

as expected for a Poisson process. The mean squared time interval is

$$\langle t^2 \rangle = \frac{2}{\lambda^2} = 2\langle t \rangle^2 \quad (7.41)$$

And the standard deviation of the time interval is equal to the mean,

$$\left(\langle t^2 \rangle - \langle t \rangle^2 \right)^{1/2} = \langle t \rangle \quad (7.42)$$

It is found for the Poisson distribution which describes bacterial motion, that the apparent diffusion coefficient (D) is given by

$$D = \frac{v^2 \tau}{3(1-\alpha)} \quad (7.43)$$

where α is the mean value of the cosine between successive runs, v is the velocity at which the bacterium propels itself and τ is the mean duration of the straight runs. If the mean angle between successive runs is zero ($\alpha=0$) the apparent diffusion coefficient is $D=v^2\tau/3$, which is identical to the result for unbiased translational diffusion.

Figure 7.11 shows the range of velocities at which cells can propel themselves at. These motile processes fulfil a diverse range of functions such as to search for food or to explore a new ecological niche, but also

many other more sophisticated tasks require motility such as when nerve cells are plugged into muscle tissue during morphogenesis or sound waves in the cochlea of the mammalian ear are detected by active cilial oscillations.

Cells employ a range of unusual strategies and gaits to propel themselves around (**figure 7.12**). Ameoboid type motion is observed with many mammalian cells at surfaces (an active gel on the cell periphery causes protrusions of the membrane that results in global motion), cilia rotate around in helical waves (metrachronal waves) along some microorganisms and similarly the internal area of many mammalian organs is covered with cilia to clear airways, move embryos and pump fluids. Some bacteria are helical in shape and follow a cork screw motion. Algae can have a comb-like appendage that they hold in front of themselves and are unusual in that they can pull themselves through the fluid (E.coli in contrast are pushers). Crucial motile processes occur during cell division as the nucleus divides and the mitotic spindle contracts (**Chapter 16**). Other examples of cellular motility include the gas vesicle mediated motion of bacteria in the sea. Gas vesicles allow them to modify their buoyancy and thus to move vertically. Pili allow some bacteria to crawl across surfaces in an analogous manner to tanks on tank treads.

7.4) First passage problem

The first passage problem is a basic question in the statistical physics of biological processes. It asks, what is the time for a particle to travel a certain distance for the first time? Events that exceed the threshold distance and then return to it are not included in the calculation. It is particularly important for transport processes involved in chemical reactions, since the reaction rate is determined by the first passage time, but it also provides a useful statistical measure to quantify motility processes in addition to the mean square displacement, and the kurtosis of the displacement (**Section 7.6**). The diffusion limited rate of a first passage process is thus the reciprocal of the first passage time. For example this could be the time for a particle released at the origin ($x=0$) to be absorbed at a boundary at $x=x_0$ (**figure 7.13**). The mean time to capture (t_0) is given by

$$t_0 = \frac{1}{j(x_0)} = \frac{1}{j(x)} \qquad (7.44)$$

where $j(x)$ is the concentration flux as described in **Section 7.1**.

The solution to the reflecting wall and absorbing wall problem is plotted in **figure 7.14**. In the absence of an external force the mean first passage time is approximately just the time to diffuse in one dimension (from equation (7.7)),

$$t \approx \frac{x_0^2}{2D} \qquad (7.45)$$

More accurate expressions include the corrections for particles that arrive for the 2nd, 3rd, 4th,.. times (see Sidney Redner's book on first-passage processes).

As an example consider a 500 nm diameter protein that diffuses near a fibrin fibre. The first passage time to diffuse the distance between adjacent fibrin monomers (45 nm) is found to be 2.33×10^{-3} s, if an estimated diffusion coefficient from the Stokes Einstein equation is used (equation (7.11), $D\approx4.35\times10^{-13}\ m^2s^{-1}$). A similar calculation is useful to understand the mechanism of motion in the lac repressor along a DNA chain i.e. the time to explore the one dimensional length of a DNA chain by an enzyme (**Chapter 18**).

A more sophisticated problem is how long a molecule that is initially at the origin ($x=0$) takes to diffuse over an energy barrier placed a certain distance away (x_0). For a constant force (F) the potential (U) as a function of distance (x) is given by

$$U(x) = -Fx \qquad (7.46)$$

The first passage time (t) for the motion is found to be

$$t = 2\left(\frac{x_0^2}{2D}\right)\left(\frac{kT}{Fx_0}\right)^2\left\{e^{-Fx_0/kT} - 1 + \frac{Fx_0}{kT}\right\} \qquad (7.47)$$

Detailed examination of this expression indicates that when the diffusion is steeply downhill, the force is large and positive, and the first passage time approaches the distance divided by the average velocity (x_0/v). When the diffusion is uphill the first passage time increases approximately exponentially as the opposing force is increased (**figure 7.11**).

For the diffusion of a particle in a parabolic potential well, the first passage time (t_k, the Kramer's time) now becomes

$$t_k = b\sqrt{\frac{\pi}{4}}\sqrt{\frac{kT}{U_0}}e^{U_0/kT} \qquad (7.48)$$

where $b=\gamma/\kappa$ is the drag coefficient divided by the spring constant (**figure 7.16**) and U_0 is the height of the parabolic potential. The shape of the potential in which a particle diffuses thus sensitively affects the functional form of the first passage time.

An important example of the first passage problem considers the rate at which a protein changes its conformation. A first possible solution is provided by the *Arrhenius equation* (**figure 7.17**), which describes the transition of a protein between two states of free energy. The probability that the protein is in an activated state is given by a Boltzmann distribution. The rate constant (k_1) is therefore

$$k_1 = Ae^{-\Delta G_{al}/kT} \qquad (7.49)$$

where $\Delta G_{al}=G_a-G_1$ is the difference in energy between the two transition states (a and l). The Arrhenius equation gives no information on the constant prefactor (A) and additional assumptions are required to calculate this coefficient. In the *Eyring rate theory* the reaction constant (A) corresponds to the breakage of a single quantum mechanical vibrational bond and is typically of the order of $kT/h \approx 6*10^{12}\ s^{-1}$. This approximation applies equally well to the breakage of covalent bonds, but it is not useful for global conformational changes of protein chains.

For global protein conformational changes the *Kramers rate theory* is a more realistic calculation of the prefactor A in equation (7.45). This includes the concept of diffusive fluctuations that determine the reaction rate,

$$k_1 = \frac{\varepsilon}{\pi\tau}\sqrt{\frac{\Delta G_{al}}{kT}}e^{-\Delta G_{al}/kT} \qquad (7.50)$$

$$\Delta G_{al} = G_a - G_l \qquad (7.51)$$

Proteins diffuse into the transition state with a rate equal to the reciprocal of the diffusion time. The efficiency factor (ε) for the transition rate is equal to the probability that the conformational transition is made when in the transition state. τ is the time over which the protein's shape becomes uncorrelated. Kramer's theory indicates that the frequency factor (τ^{-1}) is approximately equal to the inverse of the relaxation time ($\tau^{-1}=\kappa/\gamma$, where κ is the elastic constant and γ is the dissipative constant for the protein).

7.5) Rate theories of chemical reactions

The rates of many biochemical processes are determined by the combined diffusion of the reactants (**Chapter 20**). It is assumed that the only interaction between biomolecules A and B in a mixture is during a collision (**figure 7.18**). The flux of matter due to molecule A, if B is at rest, is given by J_A. Fick's first equation (7.14) can be written for the flux A,

$$J_A = -D_A\frac{\partial c_A}{\partial r} \qquad (7.52)$$

where D_A is the diffusion coefficient of species A.

There is an excluded region around the two particles A and B equal to the sum of their two radii ($r_0=r_A+r_B$). Therefore for separation distances less than the radius ($r<r_0$) the concentration of A is equal to zero ($c_A=0$). For large separation distances ($r\to\infty$) the concentration of A approaches the bulk concentration ($c_A\to c_A^0$).

The total current of A that flows towards B is the flux multiplied by the area of the surface around the particle that is considered. Let dq_A/dt be the current of particles of type A over the surface area of a sphere of radius (r),

$$\frac{dq_A}{dt} = -4\pi r^2 J_A = 4\pi r^2 D_A\frac{\partial c_A}{\partial r} \qquad (7.53)$$

where equation (7.52) has been used for the flux of A particles. This expression can be simplified further by the addition of all the contributions over space to the current,

$$\frac{dq_A}{dt}\int_{r_0}^{\infty}\frac{dr}{r^2} = 4\pi D_A \int_0^{c_A^0} dc_A \qquad (7.54)$$

where r_0 is the excluded region between the particles. Integration of this variables separable equation gives

$$\frac{dq_A}{dt} = 4\pi D_A r_0 c_A^0 \qquad (7.55)$$

To calculate the total amount of complex formed per sec an additional term for B is required for the total current (dq_A/dt),

$$\frac{dq_{AB}}{dt} = 4\pi r_0 \left(D_A + D_B\right) c_A^0 c_B^0 \qquad (7.56)$$

The rate constant (k) for the reaction rate of molecules A and B that is purely due to diffusion is therefore

$$k = 4\pi f \left(D_A + D_B\right) 10^3 N r_0 \qquad (7.57)$$

where N is Avogadro's number. This expression will be used in **Chapter 18** to understand the interaction of the lac repressor with DNA.

7.6)Sub-diffusion

Inside cells, membrane pores, colloidal suspensions and generally in congested soft matter environments, thermally driven motion often does not follow the Einstein prediction for the mean square displacement on the lag time i.e. $<r^2>$ does not scale linearly as t^1, equation (7.8). Instead a subdiffusive power law is observed at short times, $<r^2> \sim t^\alpha$ where $\alpha<1$ (**figure 7.19**). The exact physical origin of the sub-diffusive motions is still being investigated. It is observed in a wide range of systems and it may have a number of physical origins. Inside cells it is likely due to a combination of diffusion in a congested environment (e.g. caging of particles by surrounding molecules), and the internal fluctuating displacements of soft molecules and aggregates e.g. the internal conformational fluctuations of polymers and membranes. Specifically, internal motions of flexible polymer chains are sub-diffusive (**Chapter 10**) which gives a molecular motivation for some of the sub-diffusive motion phenomena observed e.g. with semi-flexible cytoskeletal polymers such as actin and microtubules $<r^2> \sim t^{3/4}$. Subdiffusive motion is also observed for probes embedded in viscoelastic materials in particle tracking experiments (**Chapter 19.16**). An alternative model for subdiffusive motion is the continuous time random walk in which the wait time between each step of the motion is chosen from a fat-tailed distribution e.g. equation (3.13). Such fat-tailed distributions can be created by cage hopping of particles in congested solutions.

Confusingly, when intracellular cargoes are driven by motor protein, the activity of the motor is often superposed on the underlying thermal subdiffusive motion. A schematic diagram of the mean square displacement as a function of lag time for the driven motion of a cargo (say a vesicle propelled by kinesin or dynein along microtubules) is shown in **figure 7.19**. At short times the motion is sub-diffusive, and it switches to directed (ballistic) motion at long times.

There are a range of alternative statistical measures to analyse data in addition to the mean square displacement that provide complementary information to dissect the exact origin of sub-diffusive motion. The mean first passage time (MFPT) is a useful unbiased measure of velocity (**figure 7.20a**). Furthermore the average cosine angle between successive displacement ($<cos\theta>$) is also useful to quantify caging and directed motion, since it includes directional information, unlike the MSD or MFPT. In **figure 7.20b** $<cos\theta>$ is shown for the same system as **figure 7.19**. At short times the motion is diffusive ($\langle\cos\theta\rangle = 0$), then it becomes anti-persistent ($\langle\cos\theta\rangle < 0$) due to motion of the vesicle on the motor protein tether, and finally it becomes persistent ($\langle\cos\theta\rangle > 0$) due to continued motion in a single direction. The kurtosis of displacement fluctuations (equation (3.5)) allows the non-gaussian nature of displacement fluctuations to be probed, which is particularly useful for the analysis of constrained diffusive motion or glassy behaviour. Particle tracking can be performed with single molecules or single organisms, due to the availability of high resolution microscopes and fast sensitive cameras, which allows accurate statistical theories to be tested for many types of biomolecular and microorganism motility through the calculation of MSDs, MFPTs, angular correlations and kurtosises.

Suggested reading

If you can only read one book then try:

J.Howard, 'Mechanics of Motor Proteins and the Cytoskeleton', Sinauer, 2001. Very clear modern account of motility.

H.Berg, 'Random Walks in Biology', Princeton University Press, 1993. Classic text on biomolecular motion from an expert in the field. Much of the current chapter draws heavily on this clear exposition, which is readily readable.

S.Vogel, 'Life in moving fluids: the physical biology of flow', Princeton, 2nd edition, 1994. Classic popular account of biological hydrodynamics.

D.B.Dusenbery, 'Swimming at microscale', Havard, 2009. A popular account of cellular motility.

P.Nelson, 'Biological Physics', Freeman, 2004. Interesting introduction to statistical mechanics tools in motility.

J.Klafter and Sokolov, 'First steps in random walks', OUP, 2011. Introduction to modern mathematical techniques for random walks e.g. continuous time random walks.

D. Ben Avrahan, S.Havlin, 'Diffusion and reaction in fractals and disorder systems', CUP, 2000. More mathematical models of diffusion.

B.D. Hughes, 'Random walks and random environments', OUP, 1996. Extremely broad coverage of models for Brownian motion.

R.M.Mazo, 'Brownian motion: fluctuations, dynamics and applications', OUP, 2002. Another useful introduction to Brownian motion.

D.Bray, 'Cellular Motility: from molecules to motility', Garland Science, 2000. Classic text on cellular motility, focusing on zoological and molecular aspects.

T.Powers, E.Lauga, 'The hydrodynamics of swimming microorganisms', *Reports on Progess in Physics*, 2009, 72, 1. Excellent comprehensive discussion of the fluid mechanics of microorganism motility.

S.Redner, 'A guide to first passage processes', CUP, 2001. **Section 7.4** only considers approximate expressions for the first passage probability. More accurate results can be found in this text.

Tutorial Questions

7.1) A mosquito of length 10^{-3} m flies at a speed of 10^{-1} ms^{-1}. Calculate its Reynolds number, given that the density and dynamical viscosity of air are 1.3 kgm^{-3} and 1.8×10^{-5} Nsm^{-2} respectively.

7.2) The flow of sodium ions in a cell is assumed to satisfy Fick's law and the diffusion equation (the diffusion coefficient is 1.35×10^{-9} m^2s^{-1}). The flux of sodium is used for signalling inside an organism. Calculate how long it would take for the sodium to diffuse the length of a neuron (2.7 mm). Determine whether this is a practical mechanism of signalling.

7.3) Consider the rotational diffusion of a spherical virus. Write down an equation that relates the mean square fluctuation ($<\theta^2>$) of the virus's rotational angle to the rotational diffusion coefficient. Estimate the time for the virus to fluctuate by 90° if the thermal energy (kT) is $4.1*10^{-21}$ J, the viscosity is 0.001 Pa s and the virus can be approximated by a sphere of radius 2 μm. Calculate the time for a point on the circumference of the virus to rotate by diffusion through a distance $2\pi a$ and compare it with the time to translate by $2\pi a$.

7.4) A Poisson distribution can be used to describe the motion of a bacterium. The apparent diffusion coefficient of the bacterium is 4×10^{-6} cm^{2}s^{-1}. Calculate the average value of the cosine of the angle between consecutive runs if the cell swims at a constant speed of 1×10^{-3} cms^{-1} and the mean duration of the straight runs is one second.

Figures

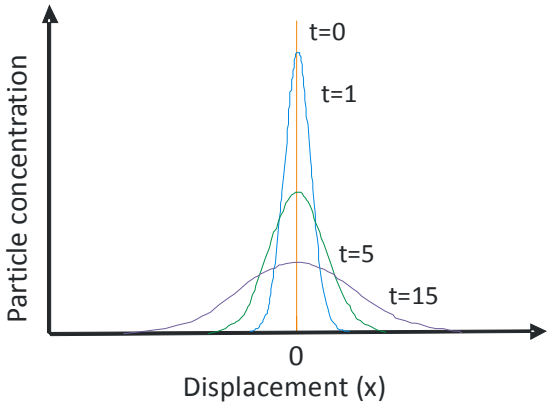

Figure 7.1. The particle concentration as a function of displacement for freely diffusing particles. The Gaussian probability distribution evolves with time. All of the particles start at *x=0*, when *t=0*.

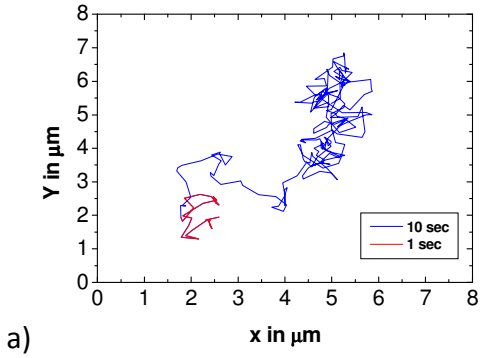

a)

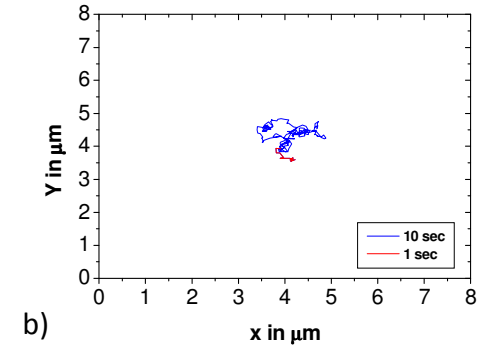

b)

Figure 7.2. Particle tracking experiments on translational diffusion using video optical microscopy. Tracks of a 0.5 µm colloidal sphere in a) water and b) glycerol for two different time periods (1 s and 10 s) are shown [*Ref, PhD A.Papagiannopoulos, University of Leeds, 2005*].

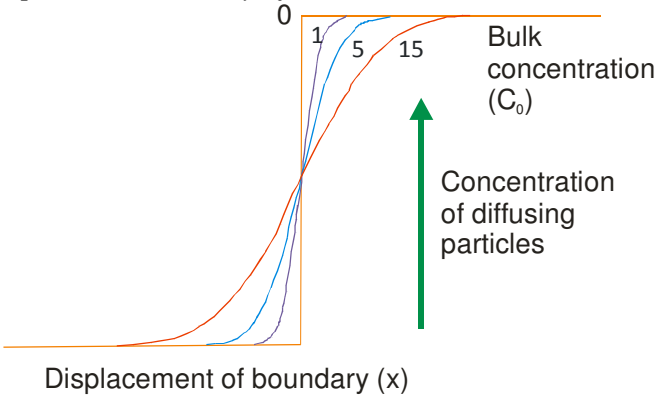

Figure 7.3. The development of the concentration gradient of a step concentration profile as a function of distance (*x*) at the times *0*, *1*, *5*, and *15* seconds, due to diffusion.

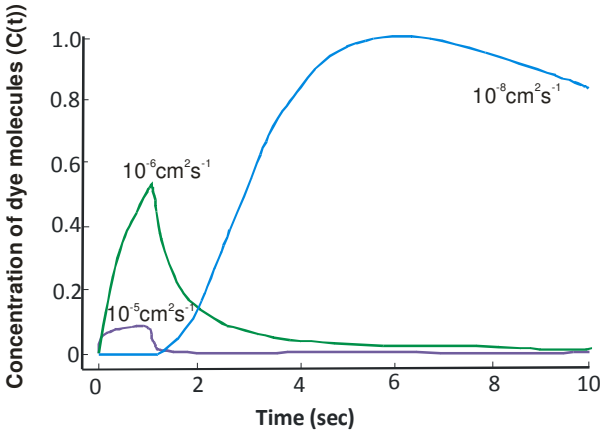

Figure 7.4. Development of the concentration profile with time (t) at a fixed position from a point source as a function of the diffusion coefficient (D) in cm^2s^{-1}. [*Ref. H.C.Berg, Random Walks in Biology, Princeton University Press, 1993*].

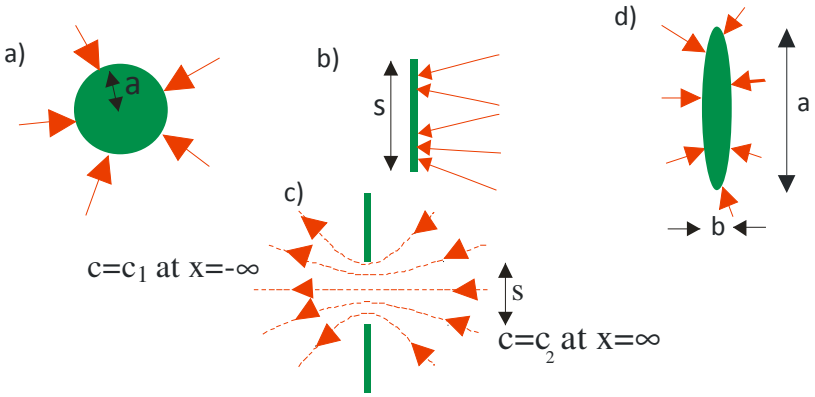

Figure 7.5. Morphologies of different absorbers for diffusing particles. a) A sphere, b) a disk, c) a circular aperture and d) an ellipsoid. Arrows indicate the motion of the diffusing species that is absorbed.

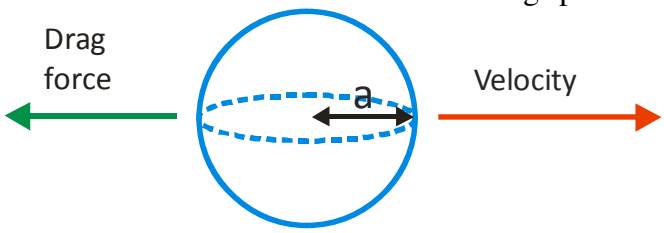

Figure 7.6. A bacterium, which approximates to a spherical colloid (radius a), experiences a drag force ($6\pi\eta av$) from the viscosity of the surrounding water which rapidly decelerates its motion. The gliding distance when no additional motile force is applied can be as small as 0.04 Å.

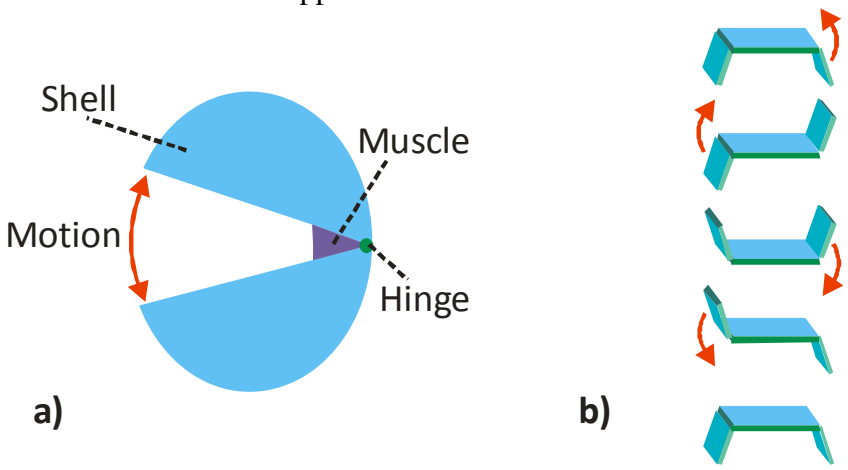

Figure 7.7. a) A scallop with a single hinge is unable to move forward at low Reynold's number due to the time reversal symmetry of the Navier-Stokes equation. b) Purcell's two hinge organism is able to propel itself forward.

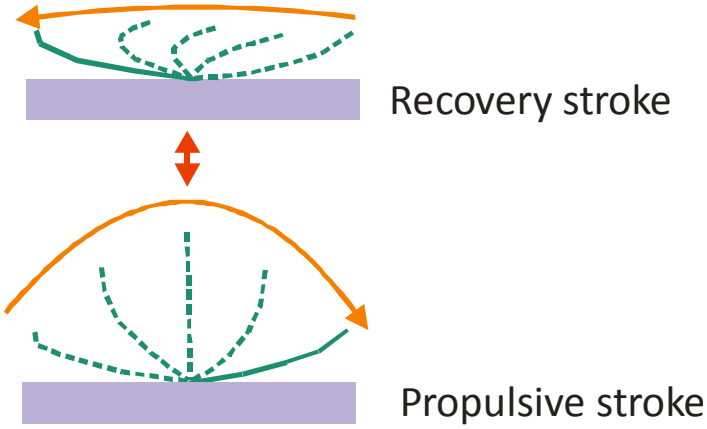

Figure 7.8. Cilia can cause propulsion by an alternation between propulsive and recovery strokes e.g. in the lungs of humans or for the motility of paramecium. The motion is not reciprocal due to the different paths of the two strokes.

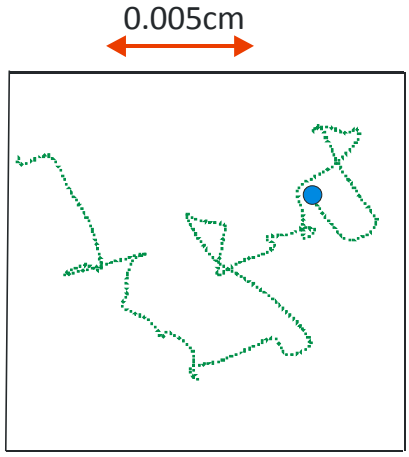

Figure 7.9. Schematic diagram of the results of a particle tracking experiment with a bacterial cell in water under an optical microscope. The trajectory describes a motility process with Poisson statistics e.g. equation (7.39) [*Ref. H.C.Berg, D.A.Brown, Nature, 1972, 239, 500-504*].

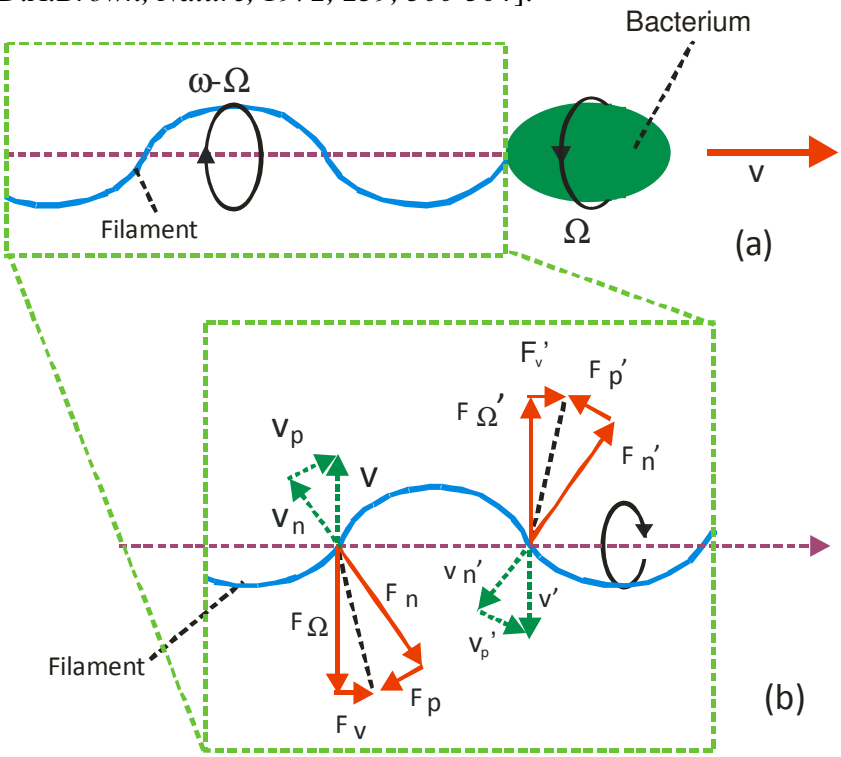

Figure 7.10. Schematic diagram of the process of bacterial locomotion a) the bacterium travels at velocity (v) and forces that propel the filament result from the component (F_v) of the viscous shear. v_n and v_p are the components of the velocity normal and parallel to the segment respectively. F_n and F_p are the force

components normal and parallel to the segment respectively. F_Ω and F_v are the components of the force parallel and perpendicular to the helical axis. The primed ' vectors correspond to another section of the filament. F_Ω and F_Ω' create a torque around the helical axis, whereas F_v and F_v' add to give the resultant thrust [*Ref. H.C.Berg, Random Walks in Biology, Princeton, 1993*].

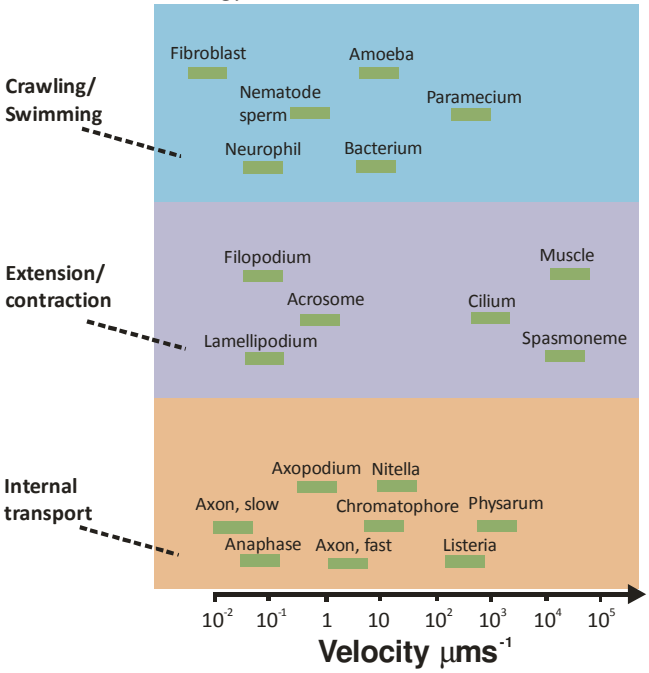

Figure 7.11. Range of velocities used for transport in cells and microorganisms. The mechanism of motility can be broadly classified as *crawling/swimming*, *extension/contraction* and *internal transport* [Ref. D.Bray, Cell movements: from molecules to motility, 2nd edition, Garland].

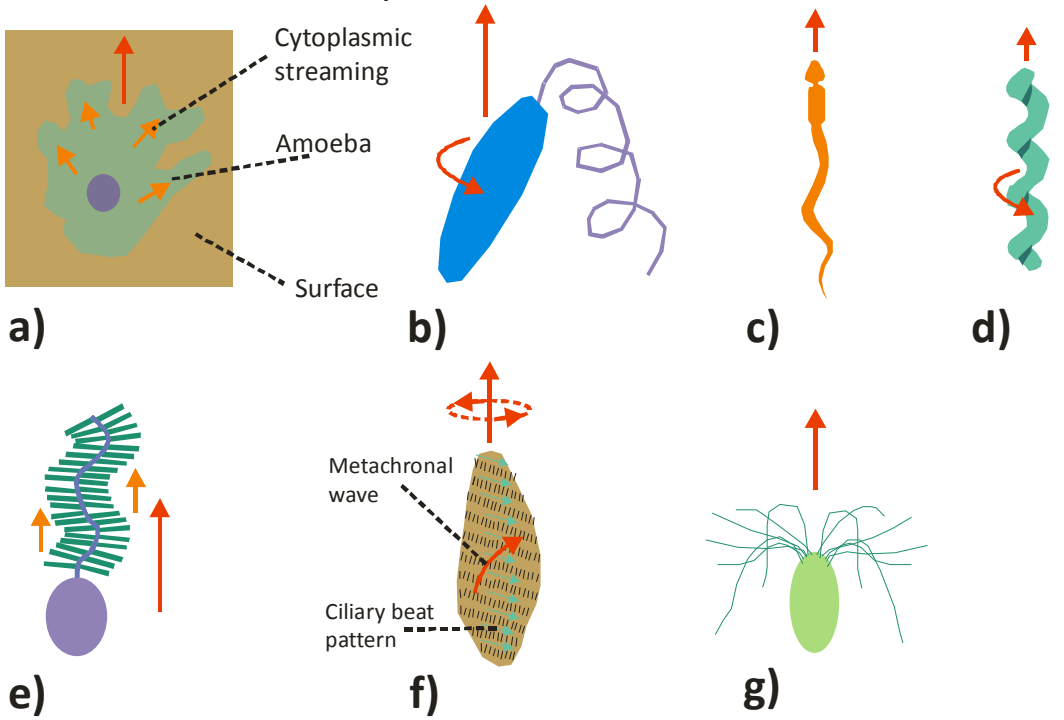

Figure 7.12. Range of different strategies used by microorganisms for motility. a) *Amoeba* use cytoplasmic streaming to crawl across a surface, b) *euglena* have a single flagellum and the cell body acts as a propeller, c) *sperm* cells use flagellae to swim, d) *spirochetes* swim using a cork screw motion, e) *chrysophytes* (golden algae) have a hairy flagellum for propulsion, f) *paramecium* use the coordinated beating of cilia in metachronal wave to propel themselves, and g) *chlamydomonas* (green algae) swim with multiple flagellae.

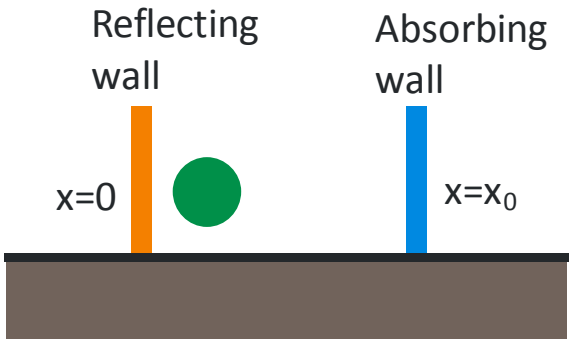

Figure 7.13. Schematic diagram of the geometry used to calculate the first passage time for a freely diffusing particle which travels from $x=0$ to an absorbing wall at $x=x_0$.

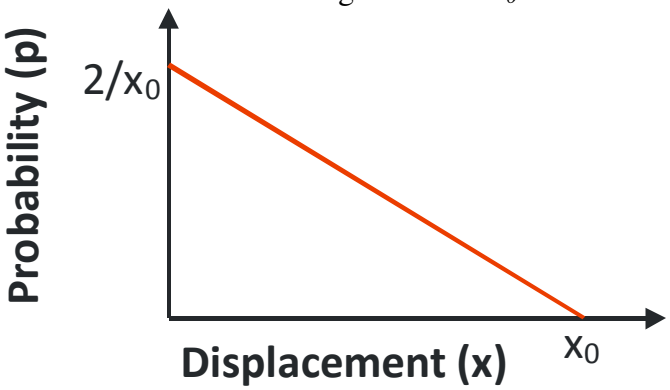

Figure 7.14. Solution of the first passage problem of a freely diffusing particle in one dimension that is placed between a reflecting wall and an absorbing wall. The probability is shown as a function of displacement (x) for the situation illustrated in **figure 7.13**.

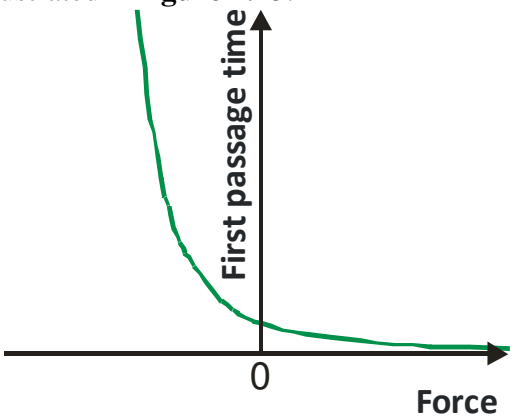

Figure 7.15. First passage time for the diffusion of a particle in one dimension as a function of the applied force, if the particle is attached to an elastic element $U(x)=(1/2)\kappa x^2$ (a harmonic potential).

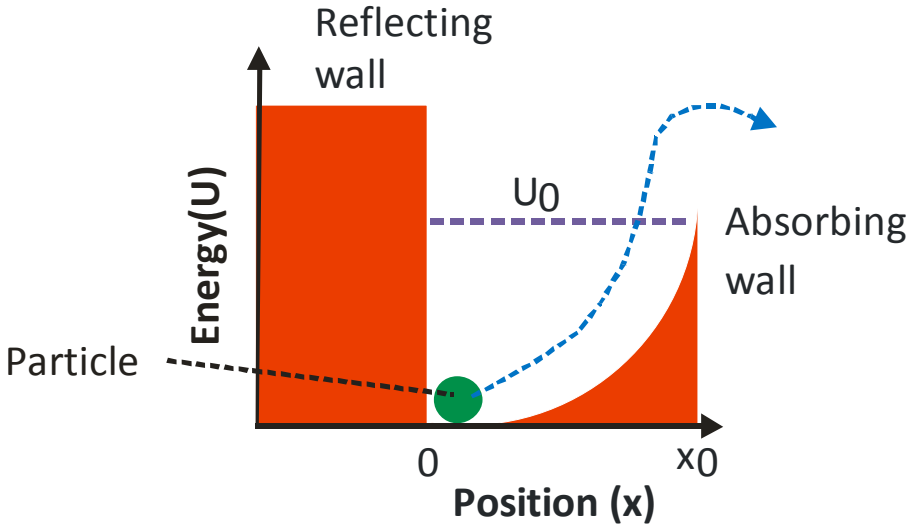

Figure 7.16. Schematic diagram that depicts the energy of a diffusing particle in one dimension as a function of position (x) that moves out of a parabolic potential well of height U_0.

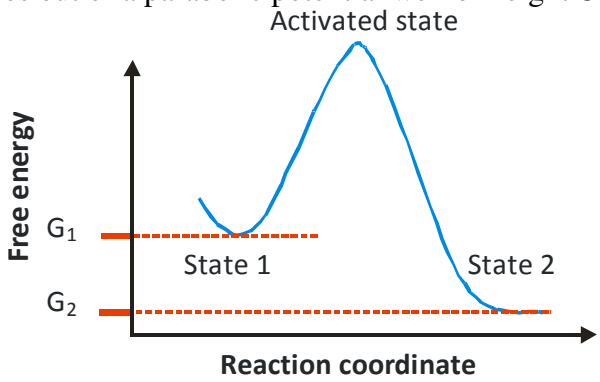

Figure 7.17. The free energy as a function of reaction co-ordinate for the conformational change of a molecule from a state *1* (free energy G_1) to a state *2* (free energy G_2).

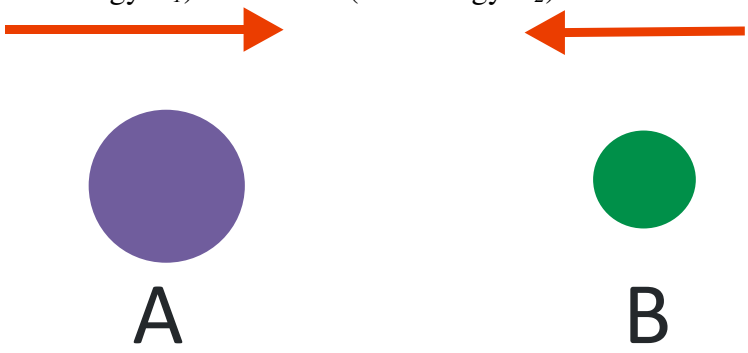

Figure 7.18. Schematic diagram of two biochemical species (A and B) that experience a collisional diffusive reaction.

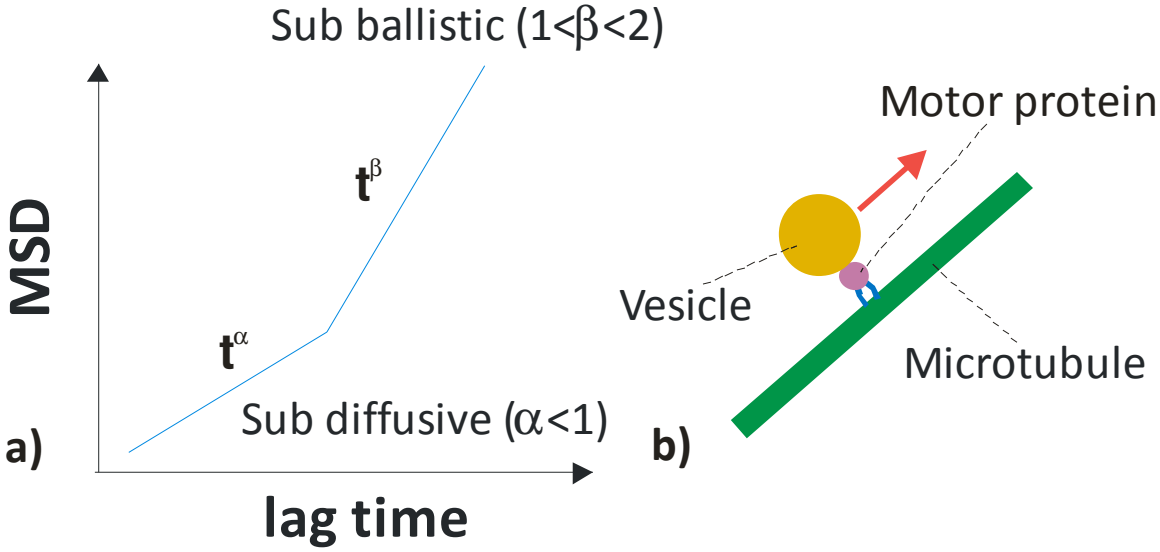

Figure 7.19.a) Mean square displacement (MSD) of a vesicle driven by a motor protein along a microtubule as a function of lag time. The motion is subdiffusive at short times ($\alpha<1$) and sub-ballistic at long times ($1<\beta<2$). b) Schematic diagram of a motor protein (dynein or kinesin) that moves a vesicle along a microtubule [Ref. A.Harrison, et al, Physical Biology, 2013, 10, 36002].

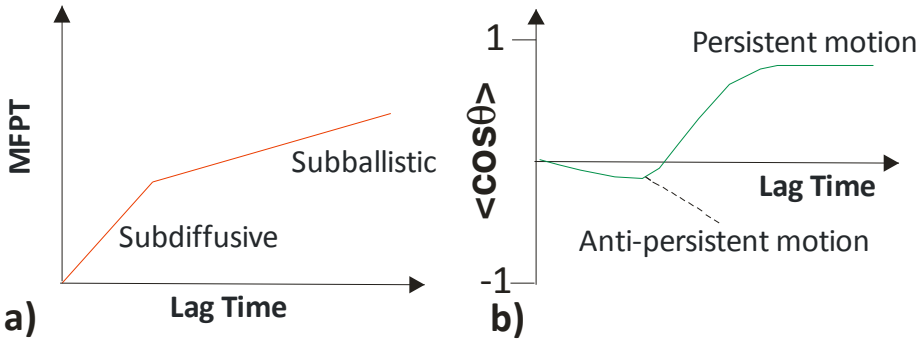

Figure 7.20. a) Mean first passage time and b) mean cosine angle between consecutive displacements, as a function of lag time for a vesicle transported by motor proteins along a microtubule. The corresponding mean square displacement is shown in **figure 7.19a** and a schematic of the vesicle is shown in **figure 7.19b** [Ref. A.Harrison, et al, Physical Biology, 2013, 10, 36002]